Phase Diagrams for the Ternary $Na_2O-Al_2O_3-H_2O$ System at (150 and 180) °C

Wei Jin,[†,‡] Shili Zheng,*[,†] Hao Du,[†] Hongbin Xu,[†] Shaona Wang,[†] and Yi Zhang[†]

National Engineering Laboratory for Hydrometallurgical Cleaner Production Technology, Key Laboratory of Green Process and Engineering, Institute of Process Engineering, Chinese Academy of Sciences, Beijing, 100190, People's Republic of China, and Graduate School of Chinese Academy of Sciences, Beijing, 100049, People's Republic of China

The full alkali concentration range phase diagrams of the $Na_2O-Al_2O_3-H_2O$ system were constructed at (150 and 180) °C. The compositions of the clear liquids and wet solid phases were analyzed by inductively coupled plasma atomic emission spectrometry (ICP-AES), and the results show that, as the Na_2O concentration increases, the Al_2O_3 solubility initially increases monotonically, to maximum values of 100 *w* (mass fraction) = 33.58 and 35.86 at (150 and 180) °C, respectively, and then decreases. At both temperatures, the solid phases were determined to be $Al_2O_3 \cdot H_2O$, $Na_2O \cdot Al_2O_3 \cdot 2.5H_2O$, $Na_2O \cdot Al_2O_3$, and NaOH by X-ray diffraction coupled with Schreinemaker's method. The phase diagrams indicate that, as the temperature increases, the $Na_2O \cdot Al_2O_3 \cdot 2.5H_2O$ phase region shrinks, while that of the $Na_2O \cdot Al_2O_3$ phase expands.

Introduction

Because of a wide application in water treatment[1] and fine chemical manufacturing technologies,[2] especially the Bayer process which has been used commercially for producing alumina-based compounds from alkali digested bauxite ores since 1897[3] in the alumina industry, the physicochemical properties of the $Na_2O-Al_2O_3-H_2O$ system have been investigated substantially over a wide range of concentrations and temperatures.

Owing to its significance, the phase diagrams of the $Na_2O-Al_2O_3-H_2O$ system, which are the fundamental data for the crucial elementary unit operations, have been intensively studied[4] by various techniques over the last two decades. Fricke and Jucaitis[5] first investigated the composition of sodium aluminate hydrate in the concentrated alkali region at 30 °C and considered the solid phase as $Na_2O \cdot Al_2O_3 \cdot 2.5H_2O$ by employing Schreinemaker's method. A subsequent argument from Kuznetsov and Dereogankin[6] suggested the solid phase to be a mixture of $Na_2O \cdot Al_2O_3 \cdot 2.5H_2O$ and $Na_2O \cdot H_2O$ using X-ray diffraction. Qiu and Chen[7] reported another new solid, $4Na_2O \cdot Al_2O_3 \cdot 12H_2O$, besides the crystalline phases mentioned above. Indeed, owing to the complexity of sodium aluminate solutions, many of the most powerful analytical techniques for investigating solution physicochemical properties such as potentiometry,[8,9] NMR,[10−12] and UV−vis spectroscopy[13] have limited success in providing useful information about such systems, as evidenced by a striking lack of agreement between analytical results obtained using these methods.[14] Thus, accurate identification of the solid phases in the $Na_2O-Al_2O_3-H_2O$ system is the subject of considerable research effort. Further, the equilibrium solid phases diversify with temperature and concentration. For example, at low concentrations, the equilibrium solid is determined to be $Al_2O_3 \cdot 3H_2O$ at (30,[4] 60,[4] 95,[15] and 110[15]) °C but becomes $Al_2O_3 \cdot H_2O$ at (130,[16] 150,[4] and 200[4]) °C. In addition, the solid transforms from $Na_2O \cdot Al_2O_3 \cdot 2.5H_2O$ to a mixture of $4Na_2O \cdot Al_2O_3 \cdot 12H_2O$ and $6Na_2O \cdot Al_2O_3 \cdot 12H_2O$ with an increase in the Na_2O concentration at 110 °C.[15] Because of equipment limitation and phase region confinement in the traditional alumina-producing process, phase diagrams at high temperatures and concentrated alkali regions are fragmentary.[4] For example, the solubility curves and crystalline phases of (150 and 200) °C are not complete, and the absence of phase diagrams between (150 and 200) °C is also an intractable problem for theoretical and practical applications.

Recently, the development of a novel diasporic bauxite digestion process,[17] which operates at about 180 °C and in concentrated alkali regions of the $Na_2O-Al_2O_3-H_2O$ system compared with 60 °C and dilute alkali regions in the traditional alumina-producing process, further addresses necessities of phase diagrams for such regions. Previous work carried out by Zhang et al. was at temperatures of (95[15] and 110[15]) °C. Five equilibrium solid phases including $Al_2O_3 \cdot 3H_2O$, $Na_2O \cdot Al_2O_3 \cdot 2.5H_2O$, $4Na_2O \cdot Al_2O_3 \cdot 12H_2O$, $6Na_2O \cdot Al_2O_3 \cdot 12H_2O$, and $Na_2O \cdot H_2O$ were reported at 95 °C, and $4Na_2O \cdot Al_2O_3 \cdot 12H_2O$ was found to be missing at 110 °C. Ma[16] et al. discovered the solid phases $Al_2O_3 \cdot H_2O$, $Na_2O \cdot Al_2O_3 \cdot 2.5H_2O$, $Na_2O \cdot Al_2O_3$, and $Na_2O \cdot H_2O$ in different alkali regions at 130 °C. To get further information for the optimization of the digestion and separation procedures in the new process, the phase diagrams at (150 and 180) °C, especially in the concentrated alkali regions, are of significant importance. In this regard, the $Na_2O-Al_2O_3-H_2O$ phase diagrams at the above-mentioned temperatures were studied over the full alkali concentration range by using X-ray diffraction coupled with Schreinemaker's method.[18]

Experimental Section

Supersaturated sodium aluminate solutions, 25 mL each, were prepared by dissolving aluminum metal (99.98 %, Merck) in hot sodium hydroxide solutions (99.99 %, Aldrich), followed by immediate filtration through a 0.22 μm pore-size membrane. All solutions were made using high purity Milli-Q water. To avoid contamination from metal containers, the solutions were

* Corresponding author. E-mail: slzheng@home.ipe.ac.cn. Fax: +86-10-62520910.
† National Engineering Laboratory for Hydrometallurgical Cleaner Production Technology.
‡ Graduate School of Chinese Academy of Sciences.

10.1021/je900859n
Published on Web 03/17/2010

Table 1. Equilibrium Data of the $Na_2O-Al_2O_3-H_2O$ System at 150 °C[a]

	composition of liquid phase (100 *w*)		composition of wet solid phase (100 *w*)		
sample no.	Na_2O	Al_2O_3	Na_2O	Al_2O_3	equilibrium crystalline phases
1	5.47	2.40			$Al_2O_3 \cdot H_2O$ (A)
2	7.76	3.81			$Al_2O_3 \cdot H_2O$ (A)
3	13.43	7.21			$Al_2O_3 \cdot H_2O$ (A)
4	15.17	10.09			$Al_2O_3 \cdot H_2O$ (A)
5	16.85	13.27			$Al_2O_3 \cdot H_2O$ (A)
6	21.16	21.43			$Al_2O_3 \cdot H_2O$ (A)
7	22.59	27.08			$Al_2O_3 \cdot H_2O$ (A)
8	24.05	33.58 (K)			$Al_2O_3 \cdot H_2O$ (A) + $Na_2O \cdot Al_2O_3 \cdot 2.5H_2O$ (B)
9	27.67	25.92	28.10	30.96	$Na_2O \cdot Al_2O_3 \cdot 2.5H_2O$ (B)
10	30.73	19.03	30.36	29.71	$Na_2O \cdot Al_2O_3 \cdot 2.5H_2O$ (B)
11	32.80	316.87	32.28	22.48	$Na_2O \cdot Al_2O_3 \cdot 2.5H_2O$ (B)
12	33.78	15.97 (L)	33.59	26.19	$Na_2O \cdot Al_2O_3 \cdot 2.5H_2O$ (B) + $Na_2O \cdot Al_2O_3$ (C)
13	37.18	11.23	37.18	19.86	$Na_2O \cdot Al_2O_3$ (C)
14	42.22	7.33	41.50	16.50	$Na_2O \cdot Al_2O_3$ (C)
15	48.69	2.94	47.37	10.33	$Na_2O \cdot Al_2O_3$ (C)
16	52.99	0.78	50.12	12.63	$Na_2O \cdot Al_2O_3$ (C)
17	58.58	0.65	56.47	7.52	$Na_2O \cdot Al_2O_3$ (C)
18	61.56	0.43 (M)			$Na_2O \cdot Al_2O_3$ (C) + NaOH (D)
19	62.38	0.00 (N)			NaOH (D)

[a] A, B, C, and D represent the solids of AlOOH, $Na_2O \cdot Al_2O_3 \cdot 2.5H_2O$, $Na_2O \cdot Al_2O_3$, and NaOH, respectively. A combination of symbols (such as A + B) means that the compounds coexist.

Table 2. Equilibrium Data of the $Na_2O-Al_2O_3-H_2O$ System at 180 °C[a]

	composition of liquid phase (100 *w*)		composition of wet solid phase (100 *w*)		
sample no.	Na_2O	Al_2O_3	Na_2O	Al_2O_3	equilibrium crystalline phases
1	6.54	4.87			$Al_2O_3 \cdot H_2O$ (A)
2	12.17	9.47			$Al_2O_3 \cdot H_2O$ (A)
3	17.21	14.74			$Al_2O_3 \cdot H_2O$ (A)
4	21.17	19.50			$Al_2O_3 \cdot H_2O$ (A)
5	24.23	28.84			$Al_2O_3 \cdot H_2O$ (A)
6	25.09	35.86 (K)			$Al_2O_3 \cdot H_2O$ (A) + $Na_2O \cdot Al_2O_3 \cdot 2.5H_2O$ (B)
7	27.35	31.12	28.09	37.29	$Na_2O \cdot Al_2O_3 \cdot 2.5H_2O$ (B)
8	29.17	27.23	29.25	30.99	$Na_2O \cdot Al_2O_3 \cdot 2.5H_2O$ (B)
9	30.82	25.82 (L)	31.07	34.31	$Na_2O \cdot Al_2O_3 \cdot 2.5H_2O$ (B) + $Na_2O \cdot Al_2O_3$ (C)
10	31.45	23.73	32.50	30.60	$Na_2O \cdot Al_2O_3$ (C)
11	35.27	18.14	35.75	29.20	$Na_2O \cdot Al_2O_3$ (C)
12	38.73	12.64	43.41	18.45	$Na_2O \cdot Al_2O_3$ (C)
13	44.95	6.33	48.32	11.58	$Na_2O \cdot Al_2O_3$ (C)
14	50.35	2.29	38.94	17.27	$Na_2O \cdot Al_2O_3$ (C)
15	52.84	0.89	51.42	6.46	$Na_2O \cdot Al_2O_3$ (C)
16	61.96	0.12 (M)			$Na_2O \cdot Al_2O_3$ (C) + NaOH (D)
17	64.00	0.00 (N)			NaOH (D)

[a] A, B, C, and D represent the solids of AlOOH, $Na_2O \cdot Al_2O_3 \cdot 2.5H_2O$, $Na_2O \cdot Al_2O_3$, and NaOH, respectively. A combination of symbols (such as A + B) means that the compounds coexist.

loaded into airtight stainless steel autoclaves with polytetrafluoroethylene linings. Finally, the autoclaves were placed in a thermostatic shaker (JFX type, Shandong Songling Chemical Equipment Co., Ltd.) with temperature control (precision 0.1 K), and the shaking speed was set to 140 rpm to accelerate the equilibrium of the complexes.

The equilibrium of the system was determined by comparing the composition of the solutions every week. After nearly one month, equilibrium was achieved, and at the experimental temperature, the viscosity of the saturated sodium aluminate solution was still low enough for easy separation of the liquid and solid phases through sedimentation for approximately 24 h. The solids obtained were washed by ethanol and then dried at 100 °C in a thermostatic oven (DHG-900 type, Jiaxing Zhongxin Chemical Equipment Co., Ltd.) for 12 h. Then the clear liquid and wet solid samples were analyzed using inductively coupled atomic plasma emission spectrometry (ICP-AES, 2400 type, Perkin-Elmer). In the Schreinemaker's method,[18] the straight line drawn through the compositions of the liquid phase and the corresponding wet solids passes through the composition of pure solid phase on a phase diagram; thus, the composition of the pure solid phase is obtained from the intersection of lines drawn through several such pairs. Besides, the solid phases were identified by X-ray diffraction (XRD) using diffraction spectrometry (Rigaku D/max-2400 X-ray with a radiation target of Cu Kα). All of the samples were scanned from 5° to 90° (2θ) range, and the results were consistent with that using Schreinemaker's method.

Results and Discussion

The equilibrium composition data of the $Na_2O-Al_2O_3-H_2O$ system at (150 and 180) °C are summarized in Table 1 and 2, and the corresponding phase diagrams are shown in Figure 1 and 2, respectively. In the figures, points A, B, C, and D represent the compositions of the equilibrium solid phases $Al_2O_3 \cdot H_2O$, $Na_2O \cdot Al_2O_3 \cdot 2.5H_2O$, $Na_2O \cdot Al_2O_3$, and $Na_2O \cdot H_2O$, respectively. Points O, K, L, M, and N are points on the saturated liquid line, while O and N represent the solubility of alumina and Na_2O in pure water, respectively.

Curves OK, KL, LM, and MN show the compositions of saturated ternary solutions with the corresponding solid phases.

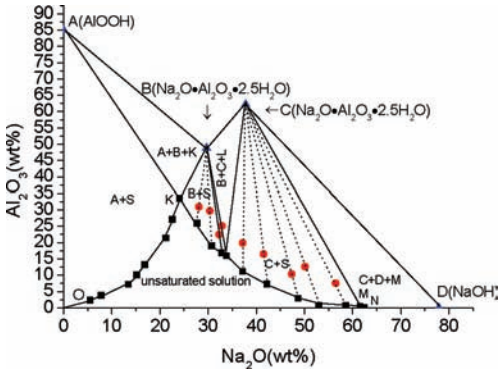

Figure 1. Phase diagram for the $Na_2O-Al_2O_3-H_2O$ system at 150 °C. A, AlOOH; B, $Na_2O \cdot Al_2O_3 \cdot 2.5H_2O$; C, $Na_2O \cdot Al_2O_3$; D, NaOH; K, L, M, three-phase points; S, saturated sodium aluminate solution; N, solubility of Na_2O in pure water at 150 °C. A combination of symbols (such as A + S) means the items coexist. OK, KL, LM, and MN indicate the composition of saturated ternary solution that in equilibrium with the solids AlOOH (A), $Na_2O \cdot Al_2O_3 \cdot 2.5H_2O$ (B), $Na_2O \cdot Al_2O_3$ (C), and NaOH (D), respectively. Thick solid lines are tie-lines between coexisting phases, and the dashed lines connect the compositions of saturated solution with the corresponding wet solid.

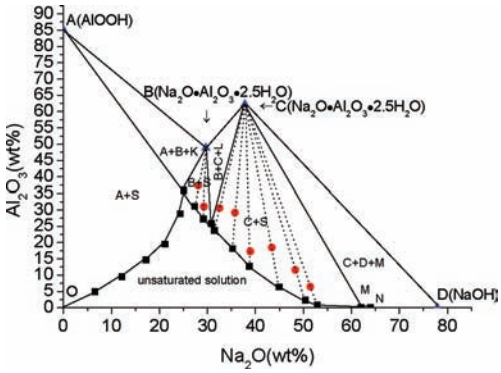

Figure 2. Phase diagram for the $Na_2O-Al_2O_3-H_2O$ system at 180 °C. A, AlOOH; B, $Na_2O \cdot Al_2O_3 \cdot 2.5H_2O$; C, $Na_2O \cdot Al_2O_3$; D, NaOH; K, L, M, three-phase points; S, saturated sodium aluminate solution; N, solubility of Na_2O in pure water at 180 °C. A combination of symbols (such as A + S) means the items coexist. OK, KL, LM, and MN indicate the composition of saturated ternary solution that in equilibrium with the solids AlOOH (A), $Na_2O \cdot Al_2O_3 \cdot 2.5H_2O$ (B), $Na_2O \cdot Al_2O_3$ (C), and NaOH (D), respectively. Thick solid lines are tie-lines between coexisting phases, and the dashed lines connect the compositions of saturated solution with the corresponding wet solid.

The data in the low concentration region at 150 °C is consistent with the results reported previously.[4] Area ABKA is a triple-phase region of $Al_2O_3 \cdot H_2O$ (A), $Na_2O \cdot Al_2O_3 \cdot 2.5H_2O$ (B), and saturated solution (K); area BCLB is for $Na_2O \cdot Al_2O_3 \cdot 2.5H_2O$ (B), $Na_2O \cdot Al_2O_3$ (C), and saturated solution (L); area CDMC is for $Na_2O \cdot Al_2O_3$ (C), NaOH (D), and saturated solution (M), while K, L, and M are three invariant points. The area above line ABCD is the all-crystalline phase region, and below the saturated liquid line OKLMN is the unsaturated sodium aluminate solution region.

Obviously, the phase diagrams show that, with an increase in the Na_2O concentration, the Al_2O_3 solubility initially increases monotonically, to the maximum values of 100 *w* (mass fraction) = 33.58 and 35.86 at (150 and 180) °C, respectively, and then decreases.

Similar to the phase diagram for the $Na_2O-Al_2O_3-H_2O$ system observed at 130 °C,[16] the equilibrium solid phases observed in this study were identified to be $Al_2O_3 \cdot H_2O$, $Na_2O \cdot Al_2O_3 \cdot 2.5H_2O$, $Na_2O \cdot Al_2O_3$, and $Na_2O \cdot H_2O$ by X-ray diffraction coupled with Schreinemaker's method. As expected, the higher the temperature, the smaller the region of the equilibrated $Na_2O \cdot Al_2O_3 \cdot 2.5H_2O$ solid is and the larger the region of $Na_2O \cdot Al_2O_3$, which suggests that in the high concentration range, as the temperature increases, the amount of sodium aluminate hydrate decreases and the $Na_2O \cdot Al_2O_3$ becomes the dominant solid phase. Besides, both $Na_2O \cdot Al_2O_3 \cdot 2.5H_2O$ (B) and $Na_2O \cdot Al_2O_3$ (C) decompose in the presence of water as suggested by the phase diagram, and the straight lines connecting the solid to the original point do not intersect with their corresponding saturated lines.

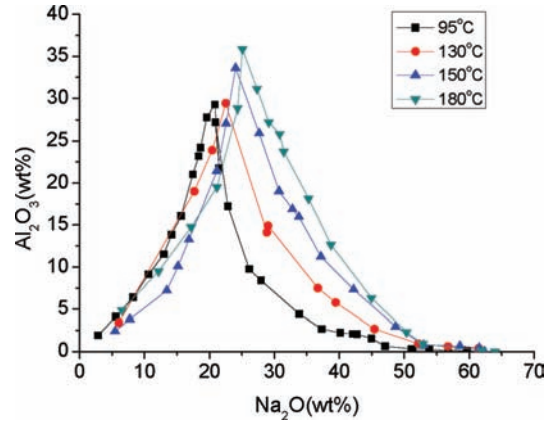

Figure 3. Solubility diagrams of the $Na_2O-Al_2O_3-H_2O$ system range from (95 to 180) °C. [Experimental data: (95[4,15] and 130[16]) °C; (150 and 180) °C, this study, see Tables 1 and 2].

The phase diagrams for the $Na_2O-Al_2O_3-H_2O$ system in the temperature range from (95 to 180) °C[15,16] are summarized in Figure 3. Clearly, with the increase of the Na_2O concentration, the Al_2O_3 solubility initially increases monotonically to a peak value and then decreases, and as the temperature increases, the maximum solubility slightly increases. Meanwhile, as the temperature increases, the equilibrium solid phase in the low Na_2O concentration region transforms from $Al_2O_3 \cdot 3H_2O$ to $Al_2O_3 \cdot H_2O$. In the high alkali region, except for $Na_2O \cdot Al_2O_3 \cdot 2.5H_2O$, other sodium aluminate hydrates gradually transform to $Na_2O \cdot Al_2O_3$.

Conclusions

Phase diagrams for the $Na_2O-Al_2O_3-H_2O$ system at (150 and 180) °C were investigated in this study. The diagrams show that, with an increase of the Na_2O concentration, the Al_2O_3 solubility initially increases monotonically, to the maximum values of 100 w = 33.58 and 35.86 at (150 and 180) °C, respectively, followed by a decrease, and this trend is also observed at other temperatures. At both temperatures, the solid phases were identified to be $Al_2O_3 \cdot H_2O$, $Na_2O \cdot Al_2O_3 \cdot 2.5H_2O$, $Na_2O \cdot Al_2O_3$, and NaOH in different concentration regions by X-ray diffraction coupled with Schreinemaker's method. Three invariant points and their relevant pairs of equilibrium solid phases ($Al_2O_3 \cdot H_2O/Na_2O \cdot Al_2O_3 \cdot 2.5H_2O$, $Na_2O \cdot Al_2O_3 \cdot 2.5H_2O/Na_2O \cdot Al_2O_3$, and $Na_2O \cdot Al_2O_3$/NaOH) were determined with their corresponding compositions. The diagrams also indicate that, as the temperature increases, the phase region of $Na_2O \cdot Al_2O_3$ expands and the region of $Na_2O \cdot Al_2O_3 \cdot 2.5H_2O$ shrinks. Meanwhile, from a comparison of the phase diagrams at other temperatures, it appears that, as the temperature increases, the equilibrium solid phase in the low Na_2O concentration region transforms from $Al_2O_3 \cdot 3H_2O$ to $Al_2O_3 \cdot H_2O$. In the high alkali region, except for $Na_2O \cdot Al_2O_3 \cdot 2.5H_2O$, other sodium aluminate hydrates gradually transform to $Na_2O \cdot Al_2O_3$.

This study fills the database gap of sodium aluminate solutions at high temperatures and concentrated alkali regions, thus providing fundamental data for optimization design of the new high-alkali digestion process.

Literature Cited

(1) Lindsay, F. K.; Ryznar, J. W. Removal of Silica from Water. *Ind. Eng. Chem. Res.* **1939**, *31* (7), 859–861.

(2) Tong, Y. C. Synthesis of Monolithic Zeolite Beta with Hierarchical Porosity Using Carbon as a Transitional Template. *Chem. Mater.* **2006**, *18*, 4218–4220.

(3) Bayer, K. J. Patent DE-PS 43977, 1887.

(4) Chen, N. Y. *Physical Chemistry of Alumina Production*; Shanghai Scientific and Technical Publishers: Shanghai, 1962.

(5) Fricke, R.; Jucaitis, P. Untersuchungen uber die Gleichgewichte in den System Al_2O_3 und $Al_2O_3 \cdot K_2O \cdot H_2O$. *Z. Anorg. Allg. Chem.* **1930**, *191*, 129–131.

(6) Kuznetsov, S. I.; Dereogankin, V. A. *Physical Chemistry of Alumina Production by Bayer Method*; Metallurgy Publishing House: Moscow, 1964.

(7) Qiu, G. F.; Chen, N. Y. Phase Study of the System Na_2O-Al_2O_3-H_2O. *Can. Metall. Q.* **1997**, *36* (2), 111–114.

(8) Plumb, R. C.; Swaine, J. W. Oxide-Coated Electrodes. II. Aluminum in Alkaline Solutions and the Nature of the Aluminate Ion. *J. Phys. Chem.* **1964**, *68*, 2057–2064.

(9) Diakonov, I.; Pokrovski, G.; Schott, J.; Castet, S.; Gout, R. An Experimental and computational study of sodium-aluminum complexing in crustal fluids. *Geochim. Cosmochim. Acta* **1996**, *60*, 197–211.

(10) Akitt, J. W.; Gessner, W.; Weinberger, M. High-field aluminium-27 nuclear magnetic resonance investigations of sodium aluminate solutions. *Magn. Reson. Chem.* **1988**, *26*, 1047–1050.

(11) Dovbysh, N. G.; Volokhov, Y. A.; Lebedev, V. B.; Sizyakov, V. M.; Mironov, V. E. Distribution of Charges in Aqueous Alkaline Solutions of Boron(III), Aluminum(III), Gallium(III), and Silicon(IV). *J. Struct. Chem.* **1981**, *22*, 137–139.

(12) Bradley, S. M.; Hanna, J. V. Aluminium-27 MAS NMR investigation of sodium aluminates formed from high pH solutions: evidence of a complex polymer containing both four- and six-coordinate aluminium. *J. Chem. Commun.* **1993**, *124*, 9–1251.

(13) Carreira, L. A.; Maroni, V. A.; Swaine, J. W.; Plumb, R. C. Raman and Infrared Spectra and Structures of Aluminate Ions. *J. Chem. Phys.* **1966**, *45*, 2216–2219.

(14) Eremin, N. I.; Volokhov, Y. A.; Mironov, V. E. Structure and Behavior of Aluminate Ions in Solutions. *Russ. Chem. Rev.* **1974**, *43*, 92–106.

(15) Zhang, Y. F.; Li, Y. H.; Zhang, Y. Phase diagram for the system Na_2O-Al_2O_3-H_2O at high alkali concentration. *J. Chem. Eng. Data* **2003**, *48*, 617–723.

(16) Ma, S. H.; Zheng, S. L.; Zhang, Y. F.; Zhang, Y. Phase diagram for the system Na_2O-Al_2O_3-H_2O at 130 °C. *J.Chem. Eng. Data* **2007**, *52*, 77–79.

(17) Zhang, Y.; Li, Z. H. Green Chemistry of Chromate Cleaner Production. *Chin. J. Chem.* **1999**, *17*, 258–266.

(18) Schott, H. A mathematical extrapolation for the methods of wet residues. *J. Chem. Eng. Data* **1961**, *6*, 324–324.

Received for review October 20, 2009. Accepted March 5, 2010. Financial support from National Natural Science Foundation of China under Grant No. 50874099, the National Basic Research Development Program of China (973 Program) under Grant No. 2009CB219901 and 2007CB613501, and Chinese Academy of Sciences Knowledge Innovation Program under Grant No. KGCX2-YW-321-2 is gratefully acknowledged.

JE900859N